Brain Tumor Pathology (2019) 36:20–26
https://doi.org/10.1007/s10014-018-0333-0

CASE REPORT

A rapidly fatal intracranial anaplastic hemangiopericytoma with de-novo dedifferentiation: emphasis on diagnostic recognition, molecular confirmation and discussion on treatment dilemma

N. J. H. Tan[1] · I. S. Y. Sun[2] · S. W. Low[2] · C. H. Kuick[3] · K. T. E. Chang[3] · C. L. Tan[1]

Received: 19 November 2018 / Accepted: 19 December 2018 / Published online: 2 January 2019

Abstract

Solitary fibrous tumors/ hemangiopericytomas (SFT/HPC) are mesenchymal tumors that share a common genetic aberration and very rarely undergo dedifferentiation. We report a unique case of an intracranial anaplastic SFT/HPC with de-novo dedifferentiation, which pursued a rapidly fatal clinical course in a 41-year-old lady. The dedifferentiated component comprised a focal area of glandular formation with epithelial immunophenotype acquisition. The distinct biphasic pattern of the tumor imparted great diagnostic challenges to the pathologists. An increased awareness of SFT/HPCs with a diverse morphologic spectrum or even a biphasic histologic pattern is essential in working up such cases. We first attempted gamma knife radiosurgery in treating a recurrent dedifferentiated SFT/HPC; unfortunately it was to no avail. Although it is now known that SFT/HPC is characterized by *NAB2-STAT6* gene fusion, the unavailability of targeted therapy against this molecular signature still results in a treatment dilemma.

Keywords Solitary fibrous tumor · Hemangiopericytoma · STAT6 · Intracranial · Dedifferentiation · Gamma knife

Introduction

Dedifferentiation in a solitary fibrous tumor/ hemangiopericytoma (SFT/HPC) is an exceptionally rare phenomenon, first recognized by Mosquera and Fletcher [1] in 2009. It is characterized by an abrupt transition from the classical spindle cell component to a high-grade, sarcomatous pattern accompanied by frequent loss of CD34 and overexpression of p53 and p16 [1]. Retroperitoneum and deep soft tissues are the most commonly affected sites [2]. Till date, there are only three intracranial examples in the literature, all of which occurred in the setting of tumor progression and recurrence, the diagnosis of which may be made relatively easier by the history and the presence of a lower grade component (Table 1) [3–5]. We report the fourth intracranial example, but the first with de-novo dedifferentiation, one that pursued a highly aggressive and rapidly fatal clinical course in a previously healthy 41-year-old lady. Our case highlights the diverse morphologic spectrum of SFT/HPCs, the value of ancillary molecular testing in the diagnostic process and the treatment dilemma associated with dedifferentiated cases.

Clinical summary

A 41-year-old female with no significant past medical history presented with a 1-month history of headache, vertiginous giddiness and unsteady gait. Clinical examination revealed signs of cerebellar dysfunction on the left side (dysmetria, dysdiadochokinesia and nystagmus). There were no cranial nerve deficits.

Computed tomography (CT) and magnetic resonance imaging (MRI) scans of the brain demonstrated a $3.6 \times 3.3 \times 2.7$ cm heterogeneously enhancing, lobulated extra-axial mass at the left cerebellopontine angle, with possible extension to the left jugular foramina (Fig. 1a). The mass exhibited no restricted diffusion or internal calcification. Vasogenic edema was noted within the left cerebellar

✉ C. L. Tan
char_loo_tan@nuhs.edu.sg

1 Department of Pathology, National University Health System, 5 Lower Kent Ridge Road, 119074 Singapore, Singapore

2 Division of Neurosurgery, Department of Surgery, Ng Teng Fong General Hospital, Singapore, Singapore

3 Department of Pathology and Laboratory Medicine, KK Women's and Children's Hospital, Singapore, Singapore

Table 1 Cases of dedifferentiated SFT/HPC of the central nervous system [3–5]

	Age/gender	Dedifferentiated component	*NAB2-STAT6* fusion	Treatment	Total duration of disease/ time when dedifferentiation occurred	Recurrence/ metastasis	Status
Maekawa et al. [4]	51/M	Pleomorphic sarcoma	*NAB2* exon 5-*STAT6* exon 18	Surgery	30 months/24 months	NA/+	Died
Moritani et al. [5]	51/F	Fibrosarcoma	NA	Surgery, radiation	58 months/44 months	+/+	Died
Lu et al. [3]	18/F	Squamous carcinoma	*NAB2* exon 6-*STAT6* exon 15	Surgery	168 months/165 months	+/−	Alive, NED
Index case	41/F	Carcinoma (adenocarcinoma)	*NAB2* exon 4-*STAT6* exon 2	Surgery, radiation, Gamma knife surgery	16 months/ at diagnosis (de-novo)	+/+	Died

NA Not available, *NED* no evidence of disease

hemisphere with consequent mass effect on the brainstem and obstructive hydrocephalus. MRI of the spine and CT scan of the thorax, abdomen and pelvis were negative for mass lesions.

The patient was stabilized with insertion of an external ventricular drain (EVD) to relieve the hydrocephalus. Thereafter, tumor resection was attempted. Intraoperative findings revealed an extremely vascular tumor which was firm and rubbery in consistency. There was no clear plane between the tumor and the brainstem tissue. The jugular foramen was not involved. Brainstem auditory evoked potentials were monitored throughout the surgery and an acute drop with minimal recovery late in the procedure prompted a halt in further debulking.

The patient recovered well following the surgery. Facial nerve function and hearing in particular were preserved on the left side. The post-operative MRI brain scan demonstrated near-total resection of the lesion (Fig. 1b). The patient was successfully weaned off the EVD and underwent adjuvant radiotherapy which was completed after 6 months.

An interval MRI scan performed 9 months after the initial resection revealed recurrence of the tumor, with associated hydrocephalus (Fig. 1c). The patient was also experiencing progressive unsteadiness of gait, speech and motor disturbances over a duration of 1 month. She underwent a ventriculoperitoneal shunt insertion to relieve the hydrocephalus, followed by a retrosigmoid decompressive craniectomy and further debulking of the tumor, performed as staged procedures over an interval of 2 weeks. Post-operative MRI imaging again demonstrated a satisfactory subtotal resection with thin tumor remnants overlying the brainstem and petrous region (Fig. 1d). She underwent gamma knife radiosurgery (GKS) to the remnant tumor 3 weeks after the debulking procedure.

Interval MRI brain scans performed 6 weeks and 3 months after GKS revealed rapid recurrence of the known lesion and multiple new lesions throughout the brain (Fig. 1e, f). An extramedullary drop metastasis at T9 level was also found. The patient died 3 months later.

Materials and methods

Both the first and second resection specimens were routinely processed for paraffin embedding and staining with hematoxylin and eosin (H&E). Immunohistochemical (IHC) staining was performed with commercially available primary antibodies, including CD34, STAT6, BCL-2, CD99, CAM5.2, AE1/AE3, MNF116, CK7, EMA, desmin, S100, SOX10 and HMB45, following the locally validated dilutions and tissue preparations. SYT break-apart fluorescence in-situ hybridization (FISH) for the detection of SYT gene rearrangement was performed using Vysis SS18 Break Apart FISH Probe Kit (Abbott Molecular, Des Plaines, IL, USA).

For targeted next-generation sequencing (NGS), total nucleic acid was extracted from formalin-fixed paraffin-embedded (FFPE) tumor tissue using the Reliaprep FFPE Total RNA Miniprep System (Promega, Wisconsin, USA). Laser microdissection of the epithelioid component was not performed. The extracted ribonucleic acid (RNA) was used for library preparation via the Archer® Fusionplex® Sarcoma Kit (AK00328), in accordance to the manufacturer's protocol. The prepared library was sequenced on the Ion Torrent PGM next-generation sequencer using the Hi-Q™ sequencing kit and Hi-Q™ OT2 kit. The results were analyzed by Archer® Data Analysis software. The extracted RNA was also subjected to one step reverse transcriptase-polymerase chain reaction (RT-PCR) using a GoTaq 1-Step RT-PCR kit (Promega). Primers-NAB2 (forward): 5′ GCA CCTACTTGTCCTCCTTG 3′; STAT6 (reverse):5′ CAG AGACATGATCTGGGACTTG 3′—flanking the breakpoint were used. The sizes of the PCR products were determined on a 2% agarose gel stained with ethidium bromide alongside a 50-bp marker (New England Biolabs, Ipswitch,

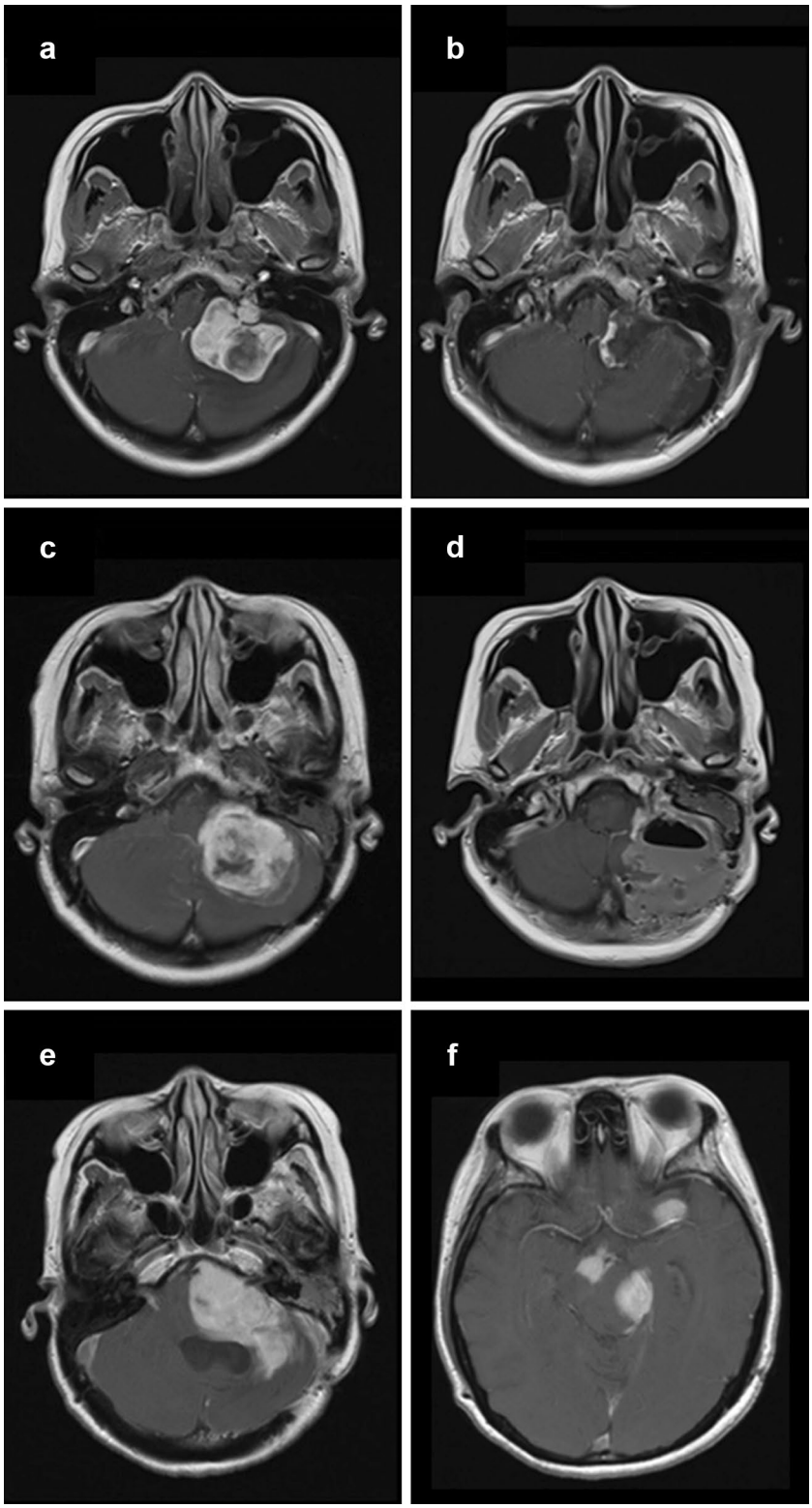

Fig. 1 Radiological features of the tumor. MRI T1 weighted image with contrast at initial presentation showing a heterogeneously enhancing, lobulated extra-axial 3.6 cm mass at the left cerebellopontine angle (**a**). Post-operative MRI brain scan following initial resection (**b**). Interval MRI brain scan 9 months after the initial resection showing tumor recurrence (**c**). Post-operative MRI brain scan following resection of recurrent tumor (**d**). Interval MRI brain scan performed 3 months after second resection and Gamma Knife Surgery showing rapid recurrence of the known lesion (**e**) and multiple new lesions (**f**)

MA, USA). The bands were excised and analyzed by Sanger sequencing using the ABI3730xl DNA sequencer (Applied Biosystems, Foster City, CA, USA) to confirm the sequence of the fusion gene.

Pathological and molecular findings

H&E sections of the first resection specimen showed a hypercellular tumor predominantly composed of dense

sheets of spindle cells with interspersed gaping vessels (Fig. 2a). The spindle cell proliferation featured scattered anaplastic and multinucleated cells, along with brisk mitotic activity (up to 29 per 10 high power fields) (Fig. 2b). Focally, there was glandular formation lined by epithelioid cells (Fig. 2c) and a tiny, discrete but unencapsulated nodule composed of epithelioid cells arranged in a nested architecture (Fig. 2d). The epithelioid cells demonstrated moderate to marked pleomorphism and possessed angulated vesicular nuclei, variably conspicuous nucleoli and abundant vacuolated cytoplasm. Up to 15 mitotic figures per 10 high-power fields were noted in the epithelioid area, including scattered atypical mitoses. The areas with epithelioid cells comprised less than 10% of the entire tumor volume. There was no other heterologous differentiation.

A Wilder's reticulin silver impregnation showed a dense pericellular reticulin deposition in the spindle cell component. Both cell types were positive for BCL-2 (Fig. 2e), CD99 and overexpressed p53. CD34 was diffusely positive in the spindle cell component but negative in the epithelioid cells (Fig. 2f). The spindle cells showed patchy reactivity for STAT6, whereas the epithelioid cells showed only

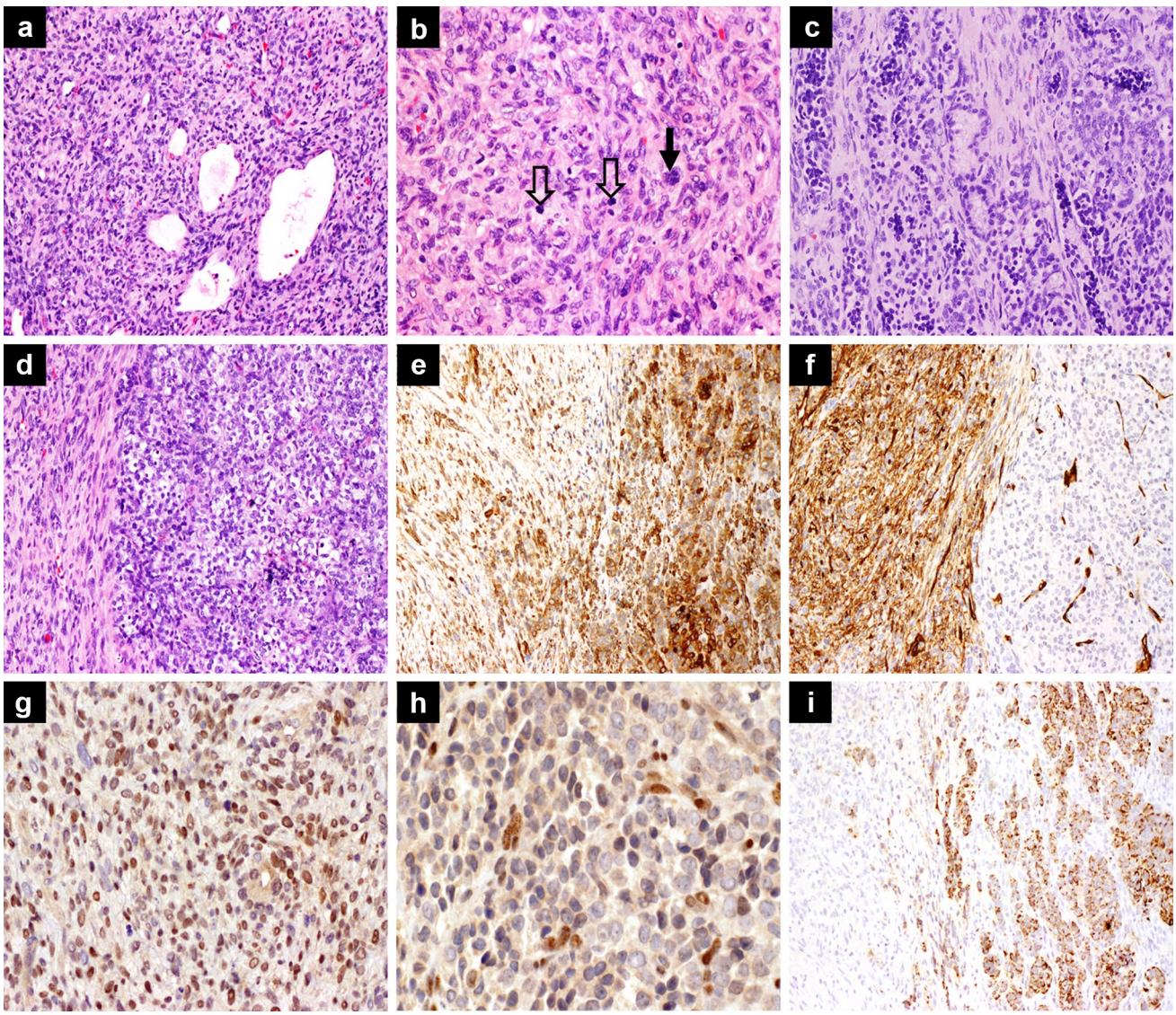

Fig. 2 Morphological and immunohistochemical features of the tumor. Tumor composed of sheets of spindle cells with variably ectatic vessels (**a**, H&E, ×100). Brisk mitotic activity (open arrows) and multinucleated cells with anaplasia (arrow) (**b**, H&E, ×400). Focally, the tumor showed glandular architecture lined by epithelioid cells (**c**, H&E, ×200). Solid nests of epithelioid tumor cells with vacuolated cytoplasm (right) and a discrete border with spindle cell component (left) (**d**, H&E, ×100). BCL-2 positivity in both spindle and epithelioid cells (**e**, ×100). CD34 was positive in the spindle cells (left) and negative in the epithelioid cells (right) (**f**, ×100). Patchy STAT6 positivity in spindle cells (**g**, ×400). Focal STAT6 positivity in epithelioid cells (**h**, ×600). CAM5.2 was positive in the epithelioid cells (right) and negative in the spindle cells (left) (**i**, ×100)

weak, focal reactivity (Fig. 2g, h). The epithelioid cells also expressed CAM5.2 (Fig. 2i). They also showed intact H3K27me3 and were negative for AE1/AE3, MNF116, CK7, EMA, desmin, S100, SOX10 and HMB45. The histological and IHC features favored an anaplastic SFT/HPC with focal epithelioid dedifferentiation. Additionally, FISH was negative for t(X,18) (SYT/SSX) translocation, precluding the differential diagnosis of a synovial sarcoma. NGS using the Archer®Fusionplex® Sarcoma kit and confirmatory RT-PCR showed a *NAB2* (exon 4)-*STAT6* (exon 2) gene fusion, clinching the diagnosis of a SFT/HPC (Fig. 3a, b).

The second resection specimen only showed the spindle cell component; no other heterologous differentiation was identified despite extensive sampling.

Discussion

An intracranial SFT/HPC with a biphasic appearance is exceedingly uncommon, illustrated by the three cases in Table 1 that demonstrated a biphasic pattern due to dedifferentiation in the setting of tumor recurrence. However, unlike those three cases, our case lacked a well-differentiated, lower grade component which may be helpful in directing us to the correct diagnosis more promptly. In addition, the discrete pattern of the epithelioid component with well-formed glandular structures compounded the diagnostic dilemma and prompted consideration of a collision tumor comprising a metastatic carcinoma and a primary mesenchymal tumor. Our case shows morphological similarities to the case reported by Pekmezci et al. [6]. These authors reported an anaplastic HPC with gland-like spaces lined by epithelioid cells that showed a similar immunoprofile to the spindle cell component and were negative for cytokeratins. Consequently, the authors considered the epithelioid cells to represent "pseudoglands" instead of tumoral dedifferentiation [6]. In contrast, the index case demonstrated an epithelioid component which formed glandular structures, showed loss of CD34 (which was retained in the spindle cell component) and acquired an epithelial characteristic, such as CAM5.2 expression. We believe that our case represents a dedifferentiated SFT/HPC, based on the loss of CD34 reactivity and acquisition of epithelial characteristics. The aggressive nature of a dedifferentiated SFT/HPC was clearly demonstrated by the cases presented by Maekawa et al. [4] and Moritani et al. [5], with both patients developing metastatic disease and dying of disease, 6 and 14 months upon the diagnoses of dedifferentiation respectively. Although the case presented by Lu et al. [3] showed no evidence of disease at the last follow-up, the duration of follow-up after the diagnosis of dedifferentiation was only 3 months. In comparison to the cases presented by Maekawa et al. [4] and Moritani et al. [5], the de-novo nature of dedifferentiation in our case imparted a highly aggressive and rapidly fatal clinical course

Fig. 3 Molecular features of the tumor. Targeted sequencing of the spindle cell component using Archer ®Fusionplex® Sarcoma Analysis kit showed fusion between NAB2 exon 4 and STAT6 exon 2 (**a**), which was confirmed with RT-PCR (**b**)

with only a 1-month history of presenting symptoms, first tumor recurrence at 3 months after completion of adjuvant radiotherapy and metastatic disease at 6 weeks after GKS. Additionally, our case demonstrated that even a minor component (< 10%) of dedifferentiation may be adequate to confer the extremely aggressive nature of the tumor and portend a highly unfavorable prognosis.

Although none is sufficiently sensitive or specific, the combination of diffuse CD34, CD99 and BCL2 positivity in the spindle cell component is a helpful clue that directs the working diagnosis towards SFT/HPC [7]. More importantly, it is now well established that SFT/HPCs are characterized by the inv12(q13q13)-derived *NAB2–STAT6* fusion with STAT6 IHC being a useful surrogate marker for this molecular signature. Since laser microdissection of the epithelioid component was not performed, the positive fusion result from NGS and RT-PCR in our case was likely represented by the spindle cell component. Nonetheless, the co-expression of STAT6 IHC in the epithelioid component, albeit focal and weak in our case, suggests that it shares a similar biological lineage with the background spindle cell component. Tumors of the central nervous system possessing a biphasic appearance are classically exemplified by gliosarcoma. Other differentials include rare cases of anaplastic meningioma with epithelial metaplasia, malignant peripheral nerve sheath tumors, metastatic carcinosarcoma and synovial sarcoma [8–15]. In approaching such cases, an increased awareness of tumors that may demonstrate a biphasic pattern, extensive tumor sampling and a judicious panel of IHC are crucial to establishing the diagnosis and excluding the mimickers. The latter step includes a diligent search for a gliomatous component in gliosarcoma, demonstration of S100 and SOX10 in neural/nerve sheath tumors, identifying a loss of H3K27me3 in malignant peripheral nerve sheath tumors, demonstration of STAT6 nuclear immunoreactivity or *NAB2-STAT6* fusion by molecular assays in SFT/HPCs, molecular analysis to detect t(X;18) in synovial sarcomas and close clinical and imaging correlation to exclude metastatic tumors.

Since its discovery in 2013, several investigators have found more than 40 *NAB2-STAT6* fusion variants and investigated the clinicopathological differences between the gene variants [16, 17]. In the meninges, the commonest fusion variant is NAB2 exon 6-STAT6 exon 16/17/18 [16]. In addition, some authors found that SFT/HPCs with this gene fusion variant tend to recur more frequently than SFT/HPCs with NAB2 exon 4-STAT6 exon 2/3, although there was no statistical correlation [16, 18, 19]. It is interesting to note that our case showed NAB2 exon 4-STAT6 exon 2 fusion, which is the variant most commonly seen in classic pleuropulmonary SFT/HPCs with diffuse fibrosis and mostly benign behavior [20, 21]. The aggressive clinical course demonstrated in our case supports the findings by other investigators that the clinical aggressiveness of extrathoracic SFT/HPCs is associated with malignant histology but unrelated to the fusion variant [17]. On a separate note, STAT6 immunoreactivity was found to be highly sensitive and specific, with most cases of SFT/HPCs showing intense and diffuse nuclear reactivity [22, 23]. Notably, the dedifferentiated SFT/HPCs have been shown to express reduced or absent STAT6 reactivity, possibly due to post-transcriptional downregulation, while retaining the fusion gene and expressing the chimeric RNA [24, 25]. The diagnostic utility of STAT6 IHC and the effect of protein downregulation in dedifferentiated tumors are best demonstrated in our case, in which the spindle cell component showed patchy and variable reactivity for STAT6 IHC while the dedifferentiated component showed only focal and weak reactivity.

The mainstay of treatment for SFT/HPC is surgical resection with negative margins. There is very limited published data regarding treatment for dedifferentiated SFT/HPC in view of its rarity. In the index case, the critical location of tumor with brainstem involvement greatly limited the potential for total surgical clearance of the tumor. In a case series of ten patients with dedifferentiated SFT/HPC, five received anthracycline-based chemotherapy and three responded [26]. This may suggest that dedifferentiated SFT/HPCs are more sensitive to chemotherapy regimens than the conventional type. Nonetheless, these ten cases were of deep soft tissue, retroperitoneum or pleuropulmonary origins. The use of anthracycline-based chemotherapy agents for intracranial tumors is hampered by the presence of the blood–brain barrier, which serves as a physical and physiological hurdle to the delivery of these drugs into the brain [27]. Few reports have described the role of GKS in treating recurrent intracranial SFT/HPCs with reasonable outcomes [28, 29]. We first attempted the use of this modality in treating a residual, recurrent SFT/HPC with dedifferentiation. Unfortunately, it was to no avail; rapid tumor recurrence and development of metastasis occurred 6 weeks upon completion of treatment. Although it is now well known that SFT/HPCs are characterized by the *NAB2-STAT6* fusion, there unfortunately remains a lack of targeted therapy against this molecular signature.

In summary, we illustrate a rare case of intracranial anaplastic SFT/HPC with biphasic histologic pattern resulting from de-novo dedifferentiation. An increased awareness of SFT/HPCs showing a diverse morphologic spectrum or even a biphasic histologic pattern is essential in working up such cases. Our case highlights the importance of diagnostic recognition, ancillary molecular genetic confirmation and the treatment dilemma in dealing with such cases. More studies are needed to evaluate the optimal treatment of this rare tumor.

Acknowledgements Targeted next generation sequencing and RT-PCR of the tumor were funded by the VIVA-KKH Paediatric Brain and Solid Tumour Programme.

Compliance with ethical standards

Conflict of interest The authors declare that they have no conflict of interest.

References

1. Mosquera J-M, Fletcher CDM (2009) Expanding the spectrum of malignant progression in solitary fibrous tumors: a study of 8 cases with a discrete anaplastic component—is this dedifferentiated SFT? Am J Surg Pathol 33:1314–1321
2. Olson NJ, Linos K (2018) Dedifferentiated solitary fibrous tumor: a concise review. Arch Pathol Lab Med 142:761–766. https://doi.org/10.5858/arpa.2016-0570-RS
3. Lu C, Alex D, Benayed R, Rosenblum M, Hameed M (2018) Solitary fibrous tumor with neuroendocrine and squamous dedifferentiation: a potential diagnostic pitfall. Hum Pathol 77:175–180. https://doi.org/10.1016/j.humpath.2017.12.024
4. Maekawa A, Kohashi K, Yamada Y, Nakamizo A, Yoshimoto K, Mizoguchi M et al (2014) A case of intracranial solitary fibrous tumor/hemangiopericytoma with dedifferentiated component. Neuropathology 35:260–265. https://doi.org/10.1111/neup.12181
5. Moritani S, Ichihara S, Hasegawa M, Takada S, Takahashi T, Kato E et al (2010) Dedifferentiation and progression of an intracranial solitary fibrous tumor: autopsy case of a Japanese woman with a history of radiation therapy of the head during infancy. Pathol Int 61:143–149. https://doi.org/10.1111/j.1440-1827.2010.02627.x
6. Pekmezci M, Vlodavsky E, Perry A (2014) Previously unrecognized pattern of central nervous system hemangiopericytoma with pseudoglandular spaces. Clin Neuropathol 33:186–189
7. Fletcher CDM, World Health Organization, International Agency for Research on Cancer (2013) WHO classification of tumours of soft tissue and bone. World Health Organization classification of tumours, 4th edn. IARC Press, Lyon
8. Marguet F, Proust F, Crahes M, Basset C, Joly-Helas G, Chambon P et al (2014) Le méningiome malin avec métaplasie adénocarcinomateuse: une entité rare à ne pas méconnaître. Ann Pathol 34:223–227. https://doi.org/10.1016/j.annpat.2014.03.004
9. Patil S, Scheithauer BW, Strom RG, Mafra M, Chicoine MR, Perry A (2011) Malignant meningiomas with epithelial (adenocarcinoma-like) metaplasia: a study of 3 cases. Neurosurgery 69:884–892. https://doi.org/10.1227/NEU.0b013e318222dc6f
10. Healy V, O'Halloran P, O'Brien S, Beausang A, Caird J (2017) CNS metastasis secondary to malignant-mixed Müllerian tumor: case report and review of therapeutics. CNS Oncol 6:315–323. https://doi.org/10.2217/cns-2017-0015
11. Voorhies J, Hattab EM, Cohen-Gadol AA (2013) Malignant peripheral nerve sheath tumor of the abducens nerve and a review of the literature. World Neurosurg 80:654–658
12. Mrowczynski O, Greiner R, Kapadia M et al (2018) Intracranial malignant peripheral nerve sheath tumor variant: an unusual neurovascular phenotype sarcoma case invading through the petrous bone. Childs Nerv Syst 34:1605–1608
13. Lin Y-J, Yang Q-x, Tian X-y, Li B, Li Z (2012) Unusual primary intracranial dural-based poorly differentiated synovial sarcoma with t(X; 18)(p11; q11). Neuropathology 33:75–82. https://doi.org/10.1111/j.1440-1789.2012.01320.x
14. Sharma S, Sharma A, Lobo G, Nayak M, Pradhan D, Samriti et al (2017) Primary dura-based synovial sarcoma of the parafalcine region of brain. Pathol Res Pract 213:868–871. https://doi.org/10.1016/j.prp.2017.03.005
15. Xiao G, Pan B, Tian X et al (2014) Synovial sarcoma in cerebellum: a case report and literature review. Brain Tumor Pathol 31:68–75
16. Nakada S, Minato H, Nojima T (2016) Clinicopathological differences between variants of the NAB2–STAT6 fusion gene in solitary fibrous tumors of the meninges and extra-central nervous system. Brain Tumor Pathol 33
17. Chuang IC, Liao K-C, Huang H-Y, Kao Y-C, Li C-F, Huang S-C et al (2016) NAB2-STAT6 gene fusion and STAT6 immunoexpression in extrathoracic solitary fibrous tumors: the association between fusion variants and locations. Pathol Int 66:288–296. https://doi.org/10.1111/pin.12408
18. Fritchie KJ, Jin L, Rubin BP, Burger PC, Jenkins SM, Barthelmeß S et al (2016) NAB2-STAT6 gene fusion in meningeal hemangiopericytoma and solitary fibrous tumor. J Neuropathol Exp Neurol 75:263–271. https://doi.org/10.1093/jnen/nlv026
19. Huang SC, Li CF, Kao YC, Chuang IC, Tai HC, Tsai JW et al (2016) The clinicopathological significance of NAB2-STAT6 gene fusions in 52 cases of intrathoracic solitary fibrous tumors. Cancer Med 5:159–168. https://doi.org/10.1002/cam4.572
20. Tai H-C, Chuang IC, Chen T-C, Li C-F, Huang S-C, Kao Y-C et al (2015) NAB2–STAT6 fusion types account for clinicopathological variations in solitary fibrous tumors. Mod Pathol 28:1324. https://doi.org/10.1038/modpathol.2015.90 https://www.nature.com/articles/modpathol201590#supplementary-information. Accessed 16 Sept 2018
21. Barthelmeß S, Geddert H, Boltze C, Moskalev EA, Bieg M, Sirbu H et al. (2014) Solitary fibrous tumors/hemangiopericytomas with different variants of the < em> NAB2- STAT6 gene fusion are characterized by specific histomorphology and distinct clinicopathological features. Am J Pathol 184:1209–1218. https://doi.org/10.1016/j.ajpath.2013.12.016
22. Yoshida A, Tsuta K, Ohno M, Yoshida M, Narita Y, Kawai A et al (2014) STAT6 Immunohistochemistry is helpful in the diagnosis of solitary fibrous tumors. Am J Surg Pathol 38:552–559
23. Doyle LA, Vivero M, Fletcher CDM, Mertens F, Hornick JL (2013) Nuclear expression of STAT6 distinguishes solitary fibrous tumor from histologic mimics. Mod Pathol 27:390. https://doi.org/10.1038/modpathol.2013.164
24. Dagrada GP, Spagnuolo RD, Mauro V, Tamborini E, Cesana L, Gronchi A et al (2015) Solitary fibrous tumors: loss of chimeric protein expression and genomic instability mark dedifferentiation. Mod Pathol 28:1074. https://doi.org/10.1038/modpathol.2015.70 https://www.nature.com/articles/modpathol201570#supplementary-information. Accessed 25 Sept 2018
25. Schneider N, Hallin M, Thway K (2016) STAT6 loss in dedifferentiated solitary fibrous tumor. Int J Surg Pathol 25:58–60. https://doi.org/10.1177/1066896916650257
26. Collini P, Negri T, Barisella M, Palassini E, Tarantino E, Pastorino U et al (2012) High-grade sarcomatous overgrowth in solitary fibrous tumors: a clinicopathologic study of 10 cases. Am J Surg Pathol 36:1202–1215. https://doi.org/10.1097/PAS.0b013e31825748f0
27. da Ros M, Iorio AL, Lucchesi M, Stival A, de Martino M, Sardi I (2015) The use of anthracyclines for therapy of CNS tumors. Anticancer Agents Med Chem 15:721–727
28. Mindermann T, Reisch R (2014) Mulitmodality management of rare solitary fibrous tumor can be associated with extended survival. Surg Neurol Int 5:S590–S592. https://doi.org/10.4103/2152-7806.148058
29. Reames DL, Mohila CA, Sheehan JP (2011) Treatment of intracranial solitary fibrous tumors with gamma knife radiosurgery: report of two cases and review of literature. Neurosurgery 69:E1023–E1028. https://doi.org/10.1227/NEU.0b013e318223b7e6 (discussion E1028)